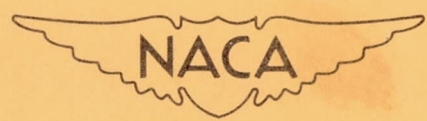# NATIONAL ADVISORY COMMITTEE FOR AERONAUTICS

TECHNICAL NOTE 2190

THE USE OF AN UNCALIBRATED CONE FOR DETERMINATION OF

FLOW ANGLES AND MACH NUMBERS AT SUPERSONIC SPEEDS

By Morton Cooper and Robert A. Webster

Langley Aeronautical Laboratory
Langley Field, Va.

NACA

Washington

March 1951

NATIONAL ADVISORY COMMITTEE FOR AERONAUTICS

———

TECHNICAL NOTE 2190

———

THE USE OF AN UNCALIBRATED CONE FOR DETERMINATION OF

FLOW ANGLES AND MACH NUMBERS AT SUPERSONIC SPEEDS

By Morton Cooper and Robert A. Webster

SUMMARY

A pressure-distribution investigation of a body of revolution has been conducted in the Langley 4- by 4-foot supersonic tunnel at a Mach number of 1.59 and a Reynolds number of 1.04×10^6 per foot. The data over the forward part of the body have been analyzed to indicate the accuracy with which an uncalibrated cone containing four static-pressure orifices and one total-pressure orifice can be used as a Mach number and flow-angle indicator at supersonic speeds. The results show that, by a simple averaging process, the free-stream Mach number for the present tests was predicted within 0.01 up to incidence angles of about 8°. Further increases in incidence resulted in the overestimation of the Mach number by as much as 0.05 at an angle of 16.10°. The angle of attack and the angle of yaw were predicted within 0.5° for various combinations of pitch and yaw up to an angle of attack of 10°. In an installation where the yaw was zero, the angle-of-attack prediction was improved to within 0.3° in the angle-of-attack range from 6° to 14° by proper orientation of the static orifices.

A comparison of the experimental pressure distributions over the surface of the cone with various theoretical calculations indicated a marked superiority of the theoretical calculations in which the presence of the entropy singularity on the upper surface of the cone was considered.

INTRODUCTION

During the past few years, appreciable effort has been expended towards the development of a suitable means for determining the free-stream Mach number and the pitch-yaw attitude of aircraft and missiles at transonic and supersonic speeds. Some of the initial efforts concerned the determination of Mach number from pitot-static tubes and also from airspeed systems using flush static-pressure orifices on fuselages in regions relatively insensitive to flight attitude. The use

of pitot-static tubes is a natural consequence of low-speed investigations
and provides a simple means for determining the Mach number through the
complete subsonic and supersonic flight range. The use of flush static-
pressure orifices, although simple in principle, yields, in reality,
only an indication of the static pressure and requires an elaborate
calibration system. In either application, the methods are restricted
to the determination of the flight Mach number since no accurate indi-
cation of the pitch-yaw attitude is inherently possible from these systems.

During investigations to develop flow-angle indicators, free-
floating vane-type angle-of-attack indicators have been evolved for use
at both subsonic and supersonic speeds. These instruments have, up to
the present time, however, been limited to the determination of angles
in a given plane.

Although many types of compact-wedge survey instruments giving both
Mach number and flow angles have been employed in supersonic wind tunnels,
the adaptation of these instruments without calibration to flight atti-
tudes is limited in the low-supersonic range by the detached-shock phenom-
enon, which restricts the incidence angles to extremely small values, and
by the mutual interference between the wedges. This interference would
invariably exist in the low-supersonic range for all wedge systems
employed to establish simultaneously the flow angles in any two perpen-
dicular planes. In order to extend the range in flight, cones having
four equally spaced radial orifices together with a total-pressure tube
at the apex have been considered as a possible means for determining Mach
number, angle of attack, and angle of yaw at supersonic speeds. Such a
scheme is indicated in reference 1 and was proposed at a later date by
Wilbur B. Huston of the Langley Aeronautical Laboratory, who suggested
the reduction of the experimental data by means of the nonlinear cone
theory of references 2 and 3.

This paper presents an analysis of the results of the pressure-
distribution measurements obtained over the forward portion of a slender
parabolic body of revolution (which was essentially conical up to the
static-pressure orifices) and indicates the accuracy with which an uncali-
brated cone, containing a total-pressure tube at the apex and four equally
spaced static-pressure orifices, can be used as a Mach number and flow-
angle indicator at supersonic speeds. The experimental data were obtained
in the Langley 4- by 4-foot supersonic tunnel in October 1949 during a
detailed investigation of the pressures over a body of revolution at a
Mach number of 1.59 and a Reynolds number of 1.04×10^6 per foot.

The results of an independent experimental investigation along these
same lines were reported in reference 4 for a much more limited appli-
cation in which the cone was yawed in a plane containing two of the
static orifices 180° apart. Such a condition presupposes, of course,

a knowledge of the plane determined by the cone axis and the relative wind - a condition which is generally unknown. Furthermore, the results indicated that the introduction of a total-pressure tube at the apex of the cone invalidated the use of the instrument as a Mach number indicator (reference 4, page 1, conclusion 3), a result which is contrary to the data obtained during the present investigation.

SYMBOLS

Free-stream conditions:

ρ mass density of air

V airspeed

a speed of sound in air

M Mach number (V/a)

μ Mach angle $\left(\sin^{-1}\frac{1}{M}\right)$

q dynamic pressure $\left(\frac{1}{2}\rho V^2\right)$

p static pressure

$r_w,\ \theta_w,\ \phi_w$ spherical polar coordinates in a wind-axis system

Cone geometry:

α angle of attack of cone axis (fig. 3)

ψ angle of yaw of cone axis (fig. 3)

ϵ incidence angle - angle between cone axis and relative wind (fig. 3)

ϕ cone radial angle (fig. 3)

θ_s cone semiapex angle

R radius of body of revolution

x   distance from apex of body of revolution measured along
                               axis of symmetry

Pressure data:

p_l local static pressure

P   pressure coefficient $\left(\dfrac{p_l - p}{q} \right)$

$\bar{p}$ pressure on surface of cone in axially symmetric flow

Subscripts:

A, C   orifice locations on opposite sides of body in plane
                               of angle of attack (fig. 3)

B, D   orifice locations on opposite sides of body in plane
                               of angle of yaw (fig. 3)

L   parameters obtained from linear theory

APPARATUS

Tunnel.- The Langley 4- by 4-foot supersonic tunnel is a rectangular,
closed-throat, single-return wind tunnel designed for a nominal Mach
number range from 1.2 to 2.2. The test-section Mach number is varied
by deflecting horizontal flexible walls against a series of fixed
interchangeable templets which have been designed to produce uniform
flow in the test section. For the present investigation, the nozzle
walls were set for a test-section Mach number of 1.59. For this Mach
number, the test section has a width of 4.5 feet and a height of 4.4 feet.
Detailed calibration studies of the flow in the test section have shown
that the general-flow properties have a relatively high degree of
uniformity as is evidenced by the values of Mach number and flow-angle
variations presented in table I. These values represent the extremes
which existed along the tunnel axis.

Model.- The test model was a parabolic body of revolution constructed
of steel to the coordinates given by the equation in figure 1(a). The
base of the model was cut off bluntly 42 inches from the apex; the fine-
ness ratio was thereby reduced from 15 to 12.2. The general arrangement
of the nose of the model, which had a semiapex angle of 7.5°, is shown
in the photograph presented in figure 1(b) and in the schematic drawing,
figure 1(a). The experimental data presented in this paper were obtained

from an apex 0.020-inch-diameter total-pressure orifice and four 0.020-inch-diameter static-pressure orifices spaced 90° around the body 1 inch from the nose. In order to install the total-pressure orifice, the nose was cut off at a diameter of approximately 0.040 inch. Hence, the ratio of the axial distance to the static-pressure orifices to the blunt-nose diameter was approximately 25.

Installation.- The model (fig. 2) was sting-supported in the tunnel and the incidence was varied in the horizontal plane. In order to define accurately the radial pressure distributions at a given axial station, the model was rotated in fixed increments to provide a much more detailed orifice coverage. The pressure tubes from the orifices were brought out from the rear of the model through the sting to multiple-tube manometers.

TESTS, CORRECTIONS, AND REDUCTION OF DATA

Tests.- The data were obtained for a range of incidence angles from 0.28° to 16.10° at a tunnel Mach number of 1.59 and a Reynolds number of 1.04×10^6 per foot. The tunnel stagnation conditions were: pressure, 0.25 atmosphere; temperature, 110° F; and dew point, -35° F. For these test conditions, the calibration data of the test section indicate that the effects of condensation on the flow over the model are probably extremely small.

Corrections.- Since the magnitudes of the flow angle, the Mach number, and the pressure gradients are small in the vicinity of the cone, no corrections for these effects have, in general, been applied to the data. For the present investigation, the cone was located in a region of the test section where the calibration indicates a Mach number of 1.60. As is shown subsequently from an examination of the experimental results, this value agrees better with the results of the present cone measurements than the nominal Mach number of 1.59 which is assumed to exist throughout the test section.

The effects of the local air-stream irregularities on the comparison of the geometric angle of attack and the angle of attack indicated by pressure measurements have been considered for the case where the correction appears to be largest, that is, at an angle of attack of 0.28°. For this condition, the effect of these irregularities would be to decrease the geometric angle of attack by about 0.08° and increase the angle of attack indicated by the pressure measurements by about 0.05°. Because of the small magnitude of these corrections, they have been neglected.

    The change in angle of the model in the horizontal plane due to
aerodynamic loading was determined by optically measuring the deflections
during the tests. This correction, although amounting to less than 0.08°
in all cases, was applied to the data. In addition to the deflections
caused by the air loads, the weight of the model introduced a small
deflection angle of 0.28° at right angles to the air loads. In presenting
the aerodynamic data, however, this droop angle was combined with the
geometrically varied angle (in a horizontal plane) to obtain the true
resultant angle which, in this paper, has been designated as the incidence
angle ϵ. (See fig. 3.) Furthermore, in all cases, the radial angle ϕ
has been geometrically referenced to the plane of the incidence angle
as required by theory.

    The accuracy of the experimental conditions, in general, is estimated
to be as follows:

Incidence angle ϵ, degrees . . . . ±0.05
Radial angle ϕ, degrees . . . . ±0.5
Radial pressure coefficient . . . . ±0.005

    Reduction of data.- The experimental pressures obtained at the
radial stations and the total-pressure orifice were reduced to Mach number,
angle of attack, and angle of yaw by applying the results of cone theory
(references 2 and 3), which have been tabulated in references 5 and 6,
together with the normal shock relations (see, for example, references 7,
8, or 9). In applying these theories, the assumption was made that the
incidence angle was small so that it could be taken directly as the vector
sum of the angle of attack and the angle of yaw. This assumption is
consistent with the limitations imposed by the cone theory (reference 3).

    In order to apply the tabulated results of references 5 and 6, the
change in slope of the body surface between the apex and the radial row
of orifices had to be neglected. In this particular application, the
curvature was small and corresponded to a slope change of $\frac{1^\circ}{4}$ in the

1-inch interval. (See equation, fig 1(a).) From linear considerations,
the variation in pressure due to the curvature was estimated to be very
small for axially symmetric flow and approximately equal in magnitude to
the experimental accuracy. Hence, the half-angle of the nose was taken
as 7.5°, a mean value which existed between the total-pressure and the
static-pressure stations.

    Since there is physically only one significant angle defining the
plane of incidence of a body of revolution with respect to the relative
wind, the incidence of the body can be varied experimentally in only one
plane and, by so doing, all possible combinations of pitch and yaw can
be obtained. The pressure readings for a conical pitot yaw head operating

at any combined pitch-yaw attitude can be obtained by geometrically
resolving the incidence data to different reference axes and by using
faired values of the basic pressures (fig. 4). This process is illus-
trated in figure 5 for a representative incidence angle of 6°. This
incidence angle can be considered as any combination of pitch and yaw
which combine to equal 6°. Then the pressures that a four-orifice system
would indicate are determined by reading pressure coefficients at

$\phi = \tan^{-1} \dfrac{\tan \psi}{\tan \alpha}$ (orifice C) and corresponding points 90° out of phase

(orifices B, A, and D). The angles of pitch and yaw then computed from
these pressures can be compared directly with the known geometric angles.
Such a method for reducing the experimental data as just outlined, however,
depends upon an accurate and detailed determination of the radial pressure
distribution. Therefore, for these tests, approximately 23 pressures
(corresponding to 46 points from symmetry conditions) were recorded to
define the radial distribution.

RESULTS AND DISCUSSION

The basic pressure-distribution data obtained on the nose of the
model have been presented in figure 4 as a function of radial position
for a range of incidence angles from 0.28° to 16.10°. Since the flow
is symmetrical with respect to the 0°, 180° axis, a folded horizontal
scale has been used; the flagged symbols designate points between 180°
and 360°. These data, together with the total pressure at the apex, have
been used to compute the free-stream Mach number and flow angles.

In the reduction of conical-pitot-yaw-head data for the prediction
of Mach numbers and flow angles at supersonic speeds, a primary problem
exists in establishing the accuracy with which theory can be used in
converting pressure measurements on the surface of a cone to the free-
stream flow parameters. Of course, if experimental calibration data,
such as shown in figure 4, are available for a particular installation,
there is no need to resort to theory for the reduction of the data.
However, in general, the amount of calibration data is limited and hence,
the theoretical reduction of the pressures will usually be necessary.
Since in the application of these theoretical methods the basic compu-
tations are extremely long and involved, the present application is
directed towards the use of the extensively tabulated cone tables presented
in references 5, 6, and 10. The tabulated results in reference 5 apply
to the case of a cone at zero yaw; reference 6 considers yaw to a first
order, and reference 10 considers yaw to a second order. In order to
interpret the experimental results more fully, the relationships obtained
from reference 6 are paralleled with reference 10 and the linear theory.

In reference 11, it has been shown that the assumption of continuous flow properties around a yawed cone (references 3, 5, 6, and 10) leads to an erroneous entropy distribution as, in reality, there is a singularity in the entropy on the top surface of the cone ($\phi = 180^\circ$). In reference 11, a correction has been introduced to account for the proper distribution of entropy at the surface of the cone. The use of this correction considerably improves the agreement between the absolute experimental and theoretical trends (as is shown subsequently); but its application, together with the complete pressure-velocity relationship used in reference 11, complicates the reduction of experimental cone measurements to flow parameters. Since in many cases, the pressure differences are not seriously impaired by the direct application of references 5 and 6, these tables are employed directly; a comparison of the flow parameters obtained by applying and neglecting the correction are presented for several special illustrations.

The pressure distribution around a slightly yawed cone as given by reference 6 is

$$p = \bar{p} + \epsilon\eta \cos \phi \qquad\qquad (1)$$

or to a higher approximation by (reference 10)

$$p = \bar{p}_\theta + \epsilon\eta_\theta \cos \phi_w + \left(p_{0_\theta} + p_{2_\theta} - 2p_{2_\theta} \sin^2\phi_w\right)\epsilon^2 \qquad (2a)$$

The pressure variation based on linear theory is given by (see reference 12, for example)

$$p_L = \bar{p}_L + \epsilon\eta_L \cos \phi + \left(1 - 4 \sin^2\phi\right)q\epsilon^2 \qquad\qquad (3)$$

In equations (1), (2a), and (3), $\bar{p}$ is the cone surface in unyawed flow; η, p_0, and p_2 represent incremental pressures due to yaw; and the subscript L indicates parameters obtained by linear considerations. In equation (2a), the added subscript θ indicates parameters evaluated on the cone surface in yawed flow, that is, at a θ value given by

$$\theta = \theta_s + \epsilon \cos \phi_w - \frac{1}{2}\epsilon^2 \cot \theta_s \sin^2\phi_w$$

The parameter ϕ_w is the radial coordinate in a spherical polar coordinate system (r_w, θ_w, ϕ_w) having the θ_w axis alined with the air stream (wind axes) and the origin located at the apex of the cone (reference 6 or 10). Although this value of ϕ_w is replaced by the radial angle ϕ on the cone in equation (1), this approximation neglects terms which have been previously retained in equation (2a); that is, the differences in the radial position coordinate in body and wind axes cannot be neglected

with consistency. However, in qualitatively discussing the experimental trends, such an approximation considerably simplified the analysis without impairing the conclusions and was therefore employed in obtaining subsequent equations (equations (5), (7b), and (9)). In order to apply equation (2a) with the tabulated range of parameters presented in reference 10, equation (2a) must be developed into a power series of the form

$$p = \bar{p} + \epsilon\eta \cos \phi_w + \epsilon^2 \left[p_0 + p_2 + \frac{1}{2} \frac{\partial^2 \bar{p}}{\partial\theta^2} + \frac{\partial\eta}{\partial\theta} - \right.$$

$$\left. \left(2p_2 + \frac{1}{2} \frac{\partial^2 \bar{p}}{\partial\theta^2} + \frac{\partial\eta}{\partial\theta} \right) \sin^2\phi_w + \ldots \right] \tag{2b}$$

where in equation (2b), the coefficients of the ϵ terms are now to be evaluated at $\theta = \theta_s$ and can be obtained from references 5, 6, and 10.

Equations (1), (2b), and (3) serve as the basis for analyzing and interpreting the Mach number and flow-angle variations. Throughout the analysis the determination of $\bar{p}$ is assumed to be sufficient to evaluate the Mach number inasmuch as $\bar{p}$, together with the total-pressure orifice reading, uniquely establishes the Mach number.

Four-Static-Orifice System

Mach number determination.- For a four-static-orifice system, $\bar{p}$ is given according to equation (1) by

$$\bar{p} = \frac{p_A + p_C}{2} \tag{4a}$$

$$\bar{p} = \frac{p_B + p_D}{2} \tag{4b}$$

where A, C and B, D represent orifices in the angle-of-attack and angle-of-yaw planes, respectively. From the more exact relationship of equation (2b), the values of $\bar{p}$ are

$$\bar{p} = \frac{p_A + p_C}{2} - \left(p_0 + p_2 + \frac{1}{2} \frac{\partial^2 \bar{p}}{\partial\theta^2} + \frac{\partial\eta}{\partial\theta} \right) \alpha^2 - \left(p_0 - p_2 \right) \psi^2 \tag{5a}$$

$$\bar{p} = \frac{p_B + p_D}{2} - \left(p_0 - p_2 \right) \alpha^2 - \left(p_0 + p_2 + \frac{1}{2} \frac{\partial^2 \bar{p}}{\partial\theta^2} + \frac{\partial\eta}{\partial\theta} \right) \psi^2 \tag{5b}$$

and the corresponding values based on linear theory (equation (3)) are

$$\bar{p}_L = \frac{p_A + p_C}{2} - q\alpha^2 + 3q\psi^2 \tag{6a}$$

$$\bar{p}_L = \frac{p_B + p_D}{2} + 3q\alpha^2 - q\psi^2 \tag{6b}$$

Hence, in the first approximation (equations (4)) the unyawed cone surface pressure is given by the average of any two static pressures 180° apart independent of the pitch-yaw attitude or the radial orientation of the orifices. The more exact relation (equations (5)) and the linear theory (equations (6)), however, show that the unyawed pressure $\bar{p}$ clearly depends upon both the angle of incidence and the radial orientation.

For small angles of incidence (α^2 and ψ^2 approaching zero), the values of $\bar{p}$ in equations (5) and (6) approach the value given by equations (4).

In order to investigate the limitations on equations (4), the Mach number was computed on the basis of the average of two pressures in the angle-of-attack plane (0°, 180°) and two pressures in the angle-of-yaw plane (90°, 270°) as the model angle of attack was increased, the yaw being held at 0°. The Mach numbers computed on this basis are presented in figure 6(a). In order to eliminate any sources of discrepancy due to angle effects on the total-pressure readings, the Mach numbers are based on both the indicated total pressure at each angle and on the total pressure for 0.28° incidence (flagged symbols). The close agreement of the Mach numbers based on both total pressures precludes the possibility of significant angle effects on the total-pressure tube. Figure 6(a) clearly shows that the Mach number and hence the average pressure of diametrically opposed orifices depends significantly upon the angle of attack and radial position; therefore, the pressure variation expressed by equation (1) and resulting in equations (4) is limited to extremely small angles, perhaps about 2° or less for this Mach number of 1.60 and cone semiapex angle of 7.5°. In this low-angle range, the predicted Mach number of 1.60 agrees very well with the local free-stream Mach number indicated during the test-section calibration. (See section on corrections.) For higher angles, the Mach number based on the 0° and 180° (C and A, respectively) orifices underestimates the true value of the free-stream Mach number; whereas, the Mach number based on the 90° and 270° (B and D, respectively) orifices considerably overestimates the free-stream Mach number. These discrepancies became prohibitive even for moderate angles of attack. A clearer interpretation of this result is possible by means of equations (5) and (6). If these equations are simplified to cover the present case and the appropriate constants are evaluated, the nonlinear values of $\bar{p}$ from equations (5) are

$$\bar{p} = \frac{p_A(180°) + p_C(0°)}{2} - 0.68q\alpha^2 \tag{7a}$$

$$\bar{p} = \frac{p_{B(90^\circ)} + p_{D(270^\circ)}}{2} + 6.17q\alpha^2 \tag{7b}$$

with the corresponding values based on the linear theory given by

$$\bar{p}_L = \frac{p_{A(180^\circ)} + p_{C(0^\circ)}}{2} - q\alpha^2 \tag{8a}$$

$$\bar{p}_L = \frac{p_{B(90^\circ)} + p_{D(270^\circ)}}{2} + 3q\alpha^2 \tag{8b}$$

From an examination of equations (7) and (8) it can be seen that, when $\bar{p}$ is based on the average of the 0° and 180° (C and A, respectively) orifices, the static pressure will be too positive and hence the Mach number will be too low as is verified by the data of figure 6(a). On the other hand, when $\bar{p}$ is based on the average of the 90° and 270° (B and D, respectively) orifices, the Mach number will be too high (the overestimation being considerably greater than the underestimation in the previous case) as is again verified by the data presented in figure 6(a). Hence the experimental results clearly indicate the importance of both incidence angle and radial position for determining the Mach number throughout the practical angle-of-incidence range.

Although attempts at using equations (5) or (6) together with an iteration procedure would undoubtedly give a better Mach number prediction than equations (4), a procedure involving the simple averaging of all four static pressures was indicated as a possible method in view of the opposing experimental trends shown in figure 6(a). (A similar procedure was used in reference 4.) The indicated Mach numbers computed on this basis are presented in figure 6(b). In order to test the validity of the method under all conceivable combinations of pitch and yaw, the four-static-orifice installation was rotated as a unit in 15° increments to cover the complete pitch-yaw range. As can be seen from figure 6(b), all pitch-yaw attitudes considered reduce to essentially one curve having a Mach number scatter of less than ± 0.009 for the complete incidence range. This average-value curve predicts the Mach number to within 0.01 up to an incidence angle of about 8°. Further increases in incidence result in the overestimation of the Mach number, the overestimation being as high as 0.05 at an incidence angle of 16°. From equations (5) and (6), respectively, the theoretical variations with incidence angle are given by second-order nonlinear theory

$$\bar{p} = \frac{p_A + p_B + p_C + p_D}{4} + 2.75q\epsilon^2 \tag{9}$$

and by linear theory

$$\bar{p} = \frac{p_A + p_B + p_C + p_D}{4} + q\epsilon^2 \qquad (10)$$

Equations (9) and (10) substantiate the reduction of the data to a
single curve which is a function of incidence angle. In both cases,
the average pressure is too low and hence the Mach number is too high
as verified by figure 6(b). Although an iteration procedure again might
yield a better approximation in the high-incidence-angle range, such a
procedure should in general be cautiously applied in view of the
limitations of the theories at the higher angles and the limited amount
of experimental data.

The accurate functioning of this system in predicting the Mach
numbers at low incidence angles is contrasted by the results reported
in reference 4 for the same free-stream Mach number. Since no systematic
evaluation tests of the two cones are available, the differences are, at
best, difficult to interpret. However, the primary difficulty encountered
in the tests reported in reference 4 may be the relatively low value of
the ratio of the axial distance to the static orifices to the blunt-nose
diameter. This parameter, which is equal to 10 for the tests of reference 4
and 25 for the present tests, is undoubtedly of primary importance and
probably depends upon both the cone angle and the free-stream Mach number.

With the determination of the Mach number, the ambient static pressure
can be calculated by the normal shock relations (references 7 to 9).

Flow-angle determination.- In the determination of the flow angles,
both the analyses for first-order (reference 6) and second-order
(reference 10) incidence angles yield the same solution if the difference
between wind and body axes is neglected. This solution is identical in
form to the linear solution.

The indicated angles of attack and angles of yaw were computed on the
basis of equation (1) and compared with the geometric angles in figure 7;
the solid lines indicate exact correlation. The combinations of pitch
and yaw selected (fig. 7) have been determined more to exploit the
limitations of the method than to select flight attitudes. In figure 7,
no yaw correlation has been presented for $\psi = 0^\circ$, because from assumed
symmetry conditions such a correlation would be exact. In each attitude
considered, the Mach number indicated by the average of the four static
pressures, for the given pitch-yaw condition, was used. This Mach number
is somewhat in error at the higher angles, but, since it will in general
be the only Mach number available for an uncalibrated instrument, it was
used in the angle prediction. The effect of this Mach number error is to
reduce the indicated angles.

In general, the agreement shown in figure 7 is surprisingly good even up to angles considerably larger than the semiapex angle. Up to an angle of attack of about 10° the maximum discrepancies are less than about 0.5°. At the higher angles, the discrepancies increase; the angle of attack generally is over-estimated whereas the angle-of-yaw discrepancies are smaller and of a more random nature. An examination of the angle-of-attack comparison in the range up to about 10° or 11° indicates that the agreement is relatively independent of pitch-yaw attitude. This fact, coupled with the excellent yaw prediction up to about 10° when the angle of attack was equal to the angle of yaw, indicates that it may be advantageous to locate the orifices in planes other than the pitch-yaw planes for high-angle-of-attack installations when the yaw is known to be small. In order to illustrate this point, the orifice system was rotated 45° as a unit and the indicated angles were resolved into the angle-of-attack plane. The results of such an installation are shown in figure 8 for unyawed flight and compared with the conventional installation. The marked superiority of the rotated installation is evident in the high-angle-of-attack range where the indicated angles are within 0.3° for angles of attack between 6° and 14°. Note, however, that such a rotated orifice system is limited to applications involving small yaw and would undoubtedly lose its advantages at larger yaw angles since the rotated system at equal pitch and yaw angles would be aerodynamically equivalent to the unrotated system in pitch alone.

In order to illustrate the effects of the correction term (reference 11) neglected in the previous analysis, the indicated angles of attack obtained from the reduction of the experimental data with and without this correction term are presented in figure 9. The data have been prepared for the case of pitch alone and for a Mach number of 1.60. The corrected angles have been obtained directly from the theoretical curve presented in figure 5 of reference 11. As can be seen from the present figure 9, the correction term has only a slight influence on the results over most of the angle range. For the highest angle, however, there is a considerable improvement. Therefore, at least for this Mach number and cone-angle range, the direct use of the tables of references 5 and 6 appears justified for most of the incidence range; for very high angles, however, an appreciable improvement can be realized by the application of the correction term.

Other Orifice Systems

Throughout the previous discussion, the analysis has been applied only to the case of a conical pitot-yaw system having four equally spaced static-pressure orifices and one total-pressure orifice. Actually, the minimum number of static orifices theoretically required for a unique solution is three. Although such a system represents a slight construction simplification, it still requires the same number of pressure readings

as the four-static-orifice system. This consideration stems from the
fact that the four-static-orifice system requires, in practice, only
four readings: a total-pressure reading, two pressure-differential
readings, and one average pressure reading. In addition, the use of a
three-orifice system introduces a much more complicated data-reduction
problem since both the pitch and yaw angles are, in general, mutually
interrelated (if two of the three orifices are not opposite each other).

Another and more serious disadvantage of the three-static-orifice
system involves the Mach number scatter with pitch-yaw attitude as shown
in figure 6. The maximum Mach number scatter at a given incidence angle
for a four-orifice system was previously pointed out to be ±0.009. This
value represents a scatter inherent in the method of data reduction and
indicates a limitation of the method of arbitrarily averaging the pressures.
For a two-orifice system (fig. 6(a)) the Mach number scatter is prohibitive
and amounts to ±0.20 from a mean value; whereas for a three-orifice system
the scatter is ±0.021. This comparison indicates that the Mach number
accuracy is clearly related to the number and probably to the radial
distribution of orifices. It is natural to question the improvements to
be expected from increasing the number of orifices from four to, say,
eight static orifices, since the scatter must diminish as the number of
orifices increase. Increasing the orifices to eight reduces the Mach
number scatter to a value of ±0.006. This value approaches a practical
limit to be expected from accidental or precision limitations on the
mechanical details of the system.

General Comments on Theoretical Prediction of

Pressure Distribution on Cone Surfaces

In order to provide a more tangible basis for understanding the
limitations of the present method and the cone theory in general, a
comparison of the theoretical pressure distributions with the experimental
data of figure 4 has been presented in figure 10. For this comparison,
the experimental pressures have been referenced to the local flow condi-
tions ($M = 1.60$) at the location of the cone. The theoretical pressure
variations predicted by equations (1) to (3) have also been presented in
this figure. In addition, the distribution corresponding to the first-
order nonlinear theory which has been corrected to the proper entropy
distribution (reference 11) is included. The numerical values of all
the parameters used are

(a) Linear theory

$$P = 0.069 + 0.526\epsilon \cos \phi + \epsilon^2(1 - 4 \sin^2\phi) \qquad (11)$$

(b) First-order nonlinear theory (reference 3)

$$P = 0.075 + 0.498\epsilon \cos \phi \qquad (12)$$

(c) Second-order nonlinear theory (reference 10)

$$P = 0.075 + 0.498\epsilon \cos \phi_w + \epsilon^2(0.675 - 6.86 \sin^2\phi_w) \qquad (13)$$

(d) First-order nonlinear theory (correction applied, reference 11)
These curves have been obtained directly from figure 5 of reference 11.

In equations (11) to (13), the incidence angle ϵ is in radians as in all previous equations. The radial coordinate ϕ_w in the wind-axis system has been converted to the body radial angle ϕ by the relationship

$$\tan \phi_w = \frac{\sin \theta_s \sin \phi}{\sin \theta_s \cos \phi \cos \epsilon + \cos \theta_s \sin \epsilon}$$

where θ_s is the cone semiapex angle.

An examination of the comparison of the experimental and theoretical results presented in figure 10 immediately indicates the marked superiority of the method of reference 11 for the complete incidence range. With the possible exception of an overestimation of the pressure minimum on the sides of the body for the highest incidence angles, the linear theory also shows relatively good agreement with the data. The inadequacy of the simple cosine variation (reference 3) becomes evident even at an angle of incidence of 4°. The second-order theory of reference 10, although improving the results at the sides of the body, distorts the pressure distribution as a whole and overcorrects on the top (approx. 140° to 170°). For the higher angles of incidence (8.05^o and 12.05^o) where the incidence is larger than the cone semiapex angle, no comparison of experiment and the second-order theory is possible.

Hence, for a Mach number of 1.60 and a cone semiapex angle of 7.5^o, the method of reference 11, and for that matter the linear theory, is better adapted to the prediction of the pressures over the body than the first- or second-order nonlinear theories of references 3 and 10, respectively. This result is probably caused by the effects of the erroneous entropy distribution as pointed out in reference 11.

For the determination of Mach number and flow angles (pressure differences), however, it appears that either the first-order nonlinear method (equation (1)) or the linear theory (equation (3)) could be used for the present combination of cone angle and Mach number. This

consideration follows in the case of the Mach number because the four
static pressures were arbitrarily averaged and the evaluation of the Mach
number depended only on the unyawed solution given in reference 2. For
the present test conditions, the linear and nonlinear solutions for the
axially symmetric case gave essentially the same result. For the deter-
mination of the flow angles, the fact that the coefficients of the
$\epsilon \cos \phi$ terms in equations (11) and (12) are approximately the same
indicates that either equation could have been used in the present case.
For the general case, however, these parameters (for both the yawed and
unyawed solutions) will diverge with increases in cone angles and changes
in Mach number, and, for large cone angles operating in the small incidence
range, the first-order nonlinear method (reference 3) would probably be
more suitable. Under extreme conditions, however, the direct application
of reference 3 for the determination of Mach number and flow angles should
be checked theoretically for several conditions with the corrected results
obtained from reference 11.

CONCLUDING REMARKS

A pressure-distribution investigation of a body of revolution has
been conducted in the Langley 4- by 4-foot supersonic tunnel at a Mach
number of 1.59 and a Reynolds number of 1.04×10^6 per foot. The data
over the forward part of the body have been analyzed to indicate the
accuracy with which an uncalibrated cone containing four static-pressure
orifices and one total-pressure orifice can be used as a Mach number and
flow-angle indicator at supersonic speeds. The results show that, by a
simple averaging process, the free-stream Mach number for the present
tests was predicted within 0.01 up to incidence angles of about 8°.
Further increases in incidence angle resulted in the overestimation of
the Mach number by as much as 0.05 at an angle of 16.10^o. The angle of
attack and the angle of yaw were predicted within 0.5^o for various combi-
nations of pitch and yaw up to an angle of attack of 10°. In an instal-
lation where the yaw was zero, the angle-of-attack prediction was improved
to within 0.3^o in the angle-of-attack range from 6° to 14° by proper
orientation of the static orifices.

A comparison of the experimental pressure distributions over the
surface of the cone with various theoretical calculations indicated the
marked superiority of the theoretical calculations when the presence of
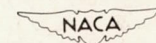the entropy singularity on the upper surface of the cone was considered.

Langley Aeronautical Laboratory
        National Advisory Committee for Aeronautics
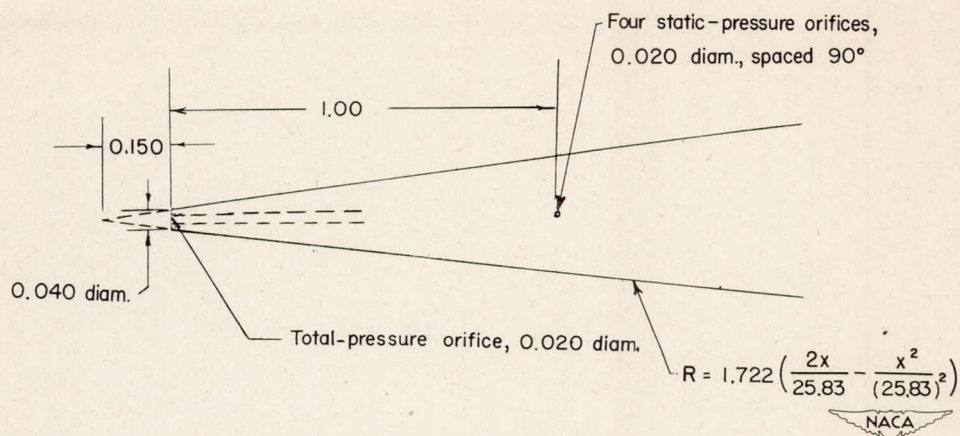   Langley Field, Va., December 12, 1950

REFERENCES

1. Ferri, Antonio: Elements of Aerodynamics of Supersonic Flows. The
     Macmillan Co., 1949, p. 98.

2. Taylor, G. I., and Maccoll, J. W.: The Air Pressure on a Cone Moving
     at High Speeds. Proc. Roy. Soc. (London), ser. A, vol. 139, no. 838,
     Feb. 1, 1933, pp. 278-311.

3. Stone, A. H.: On Supersonic Flow past a Slightly Yawing Cone.
     Jour. Math. and Phys., vol. XXVII, no. 1, April 1948, pp. 67-81.

4. Davis, Theodore: Development and Calibration of Two Conical Yawmeters.
     Meteor Rep. UAC-43, United Aircraft Corp., Oct. 1949.

5. Staff of the Computing Section, Center of Analysis (Under Direction of
     Zdeněk Kopal): Tables of Supersonic Flow around Cones. Tech Rep.
     No. 1, M.I.T., 1947.

6. Staff of the Computing Section, Center of Analysis (Under Direction of
     Zdeněk Kopal): Tables of Supersonic Flow around Yawing Cones. Tech.
     Rep. No. 3, M.I.T., 1947.

7. Burcher, Marie A.: Compressible Flow Tables for Air. NACA TN 1592,
     1948.

8. The Staff of the Ames 1- by 3-Foot Supersonic Wind-Tunnel Section:
     Notes and Tables for Use in the Analysis of Supersonic Flow.
     NACA TN 1428, 1947.

9. Emmons, Howard W.: Gas Dynamics Tables for Air. Dover Publications,
     Inc., 1947.

10. Staff of the Computing Section, Center of Analysis (Under Direction of
      Zdeněk Kopal): Tables of Supersonic Flow around Cones of Large
      Yaw. Tech. Rep. No. 5, M.I.T., 1949.

11. Ferri, Antonio: Supersonic Flow around Circular Cones at Angles of
      Attack. NACA TN 2236, 1950.

12. Allen, H. Julian: Pressure Distribution and Some Effects of Viscosity
      on Slender Inclined Bodies of Revolution. NACA TN 2044, 1950.

TABLE I

FLOW PARAMETERS ALONG TUNNEL AXIS

Distance along axis	Interval (ft)	Maximum Mach number range	Maximum horizontal-flow-angle range (deg)	Maximum vertical-flow-angle range (deg)
Test-section height times cot μ	5.5	1.585 to 1.604	-0.05 to 0.20	-0.15 to 0.30
Average model length	2.5	1.585 to 1.595	0 to 0.20	0 to 0.30

Four static-pressure orifices,
0.020 diam., spaced 90°

1.00

0.150

0.040 diam.

Total-pressure orifice, 0.020 diam.

$R = 1.722 \left(\dfrac{2x}{25.83} - \dfrac{x^2}{(25.83)^2} \right)$

NACA

(a) Schematic drawing. (All dimensions are
in inches unless otherwise indicated.)
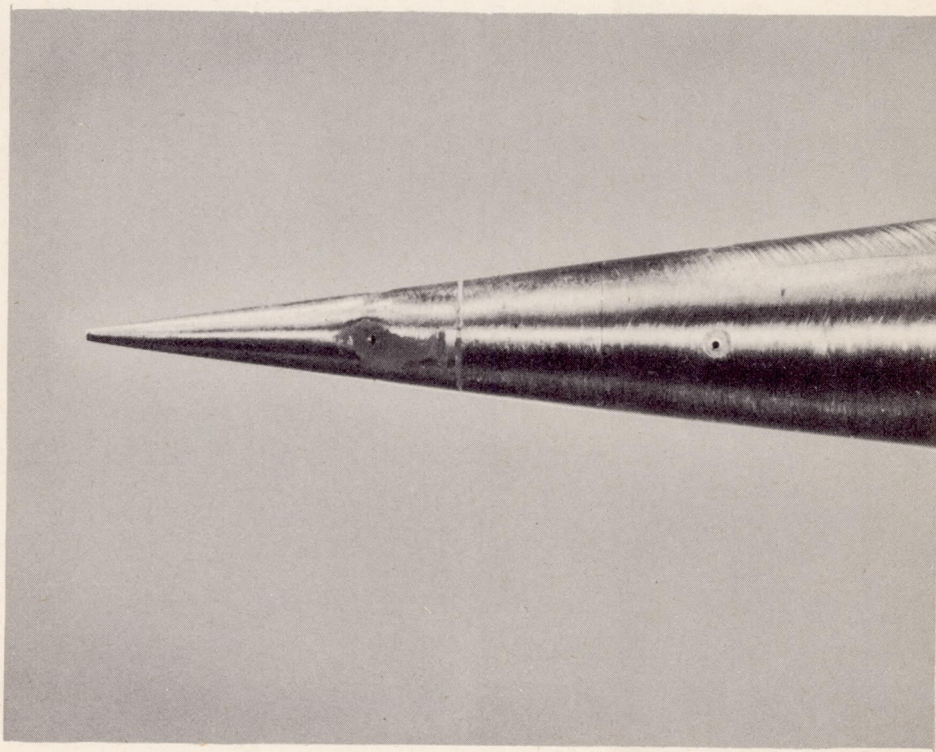
(b) Photograph of cone.   NACA
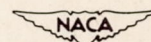
Figure 1.- Model details. Semiapex angle, 7.5°. L-63984.1
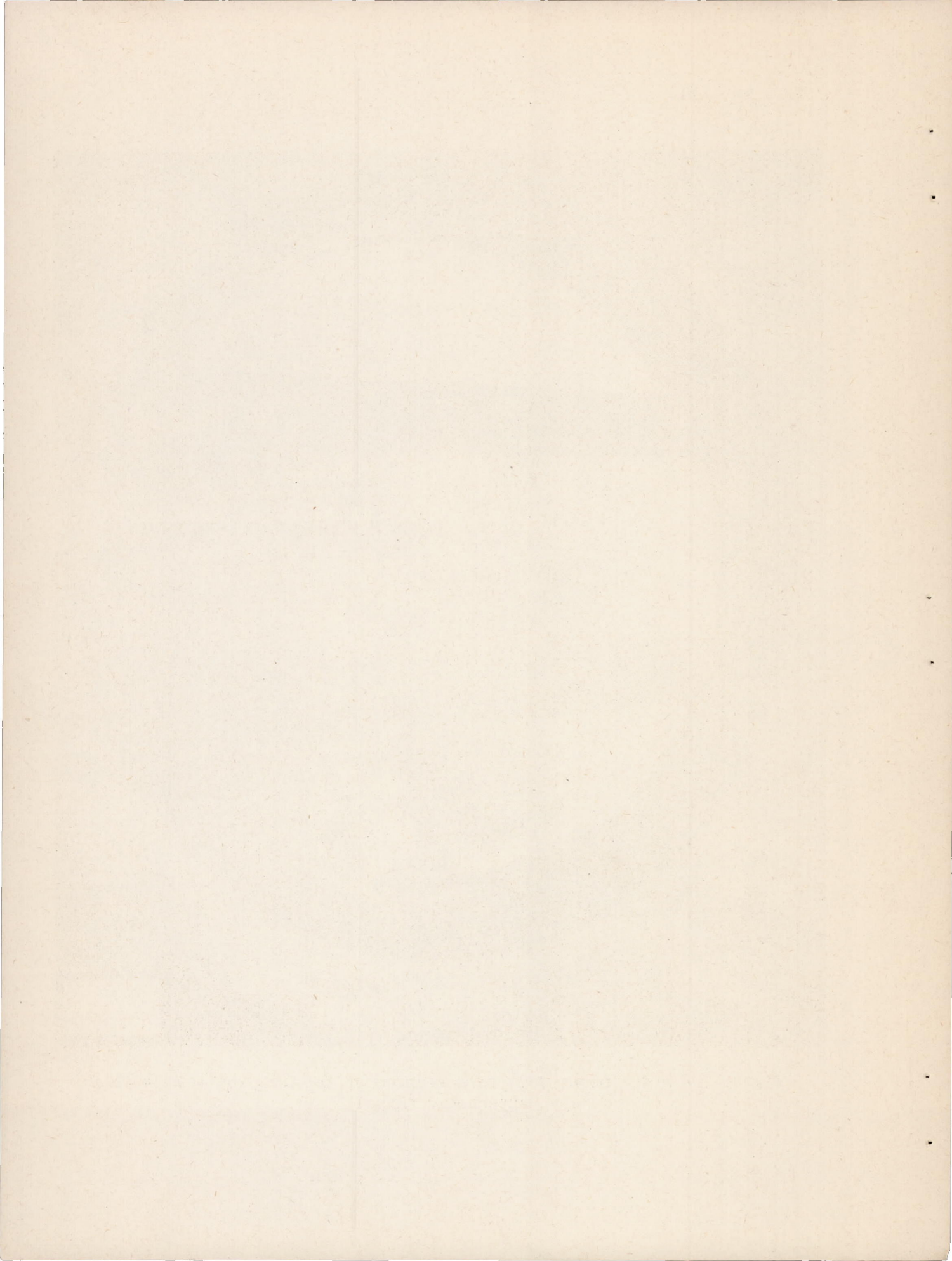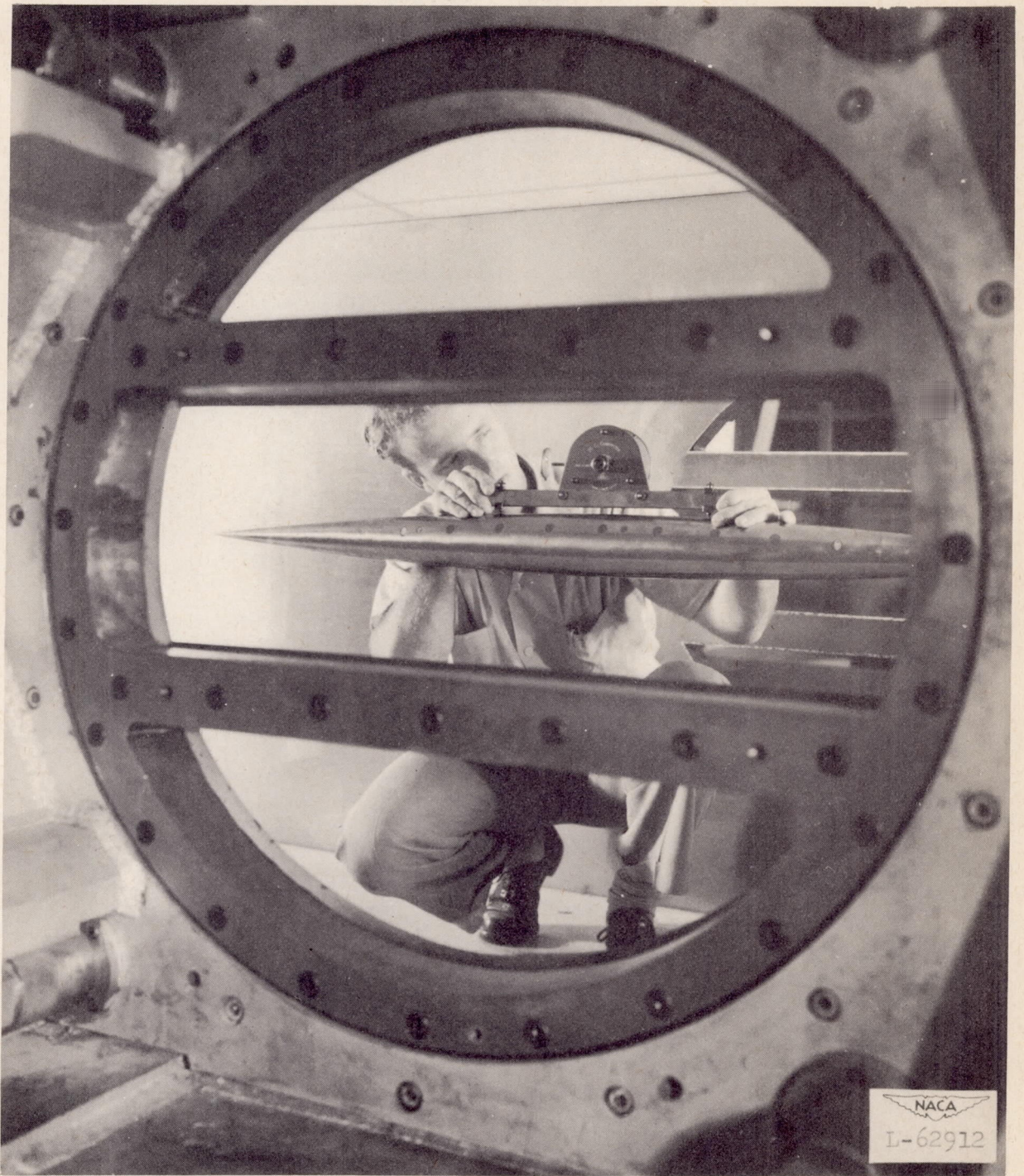
Figure 2.- Model mounted in test section of the Langley 4- by 4-foot
supersonic tunnel.
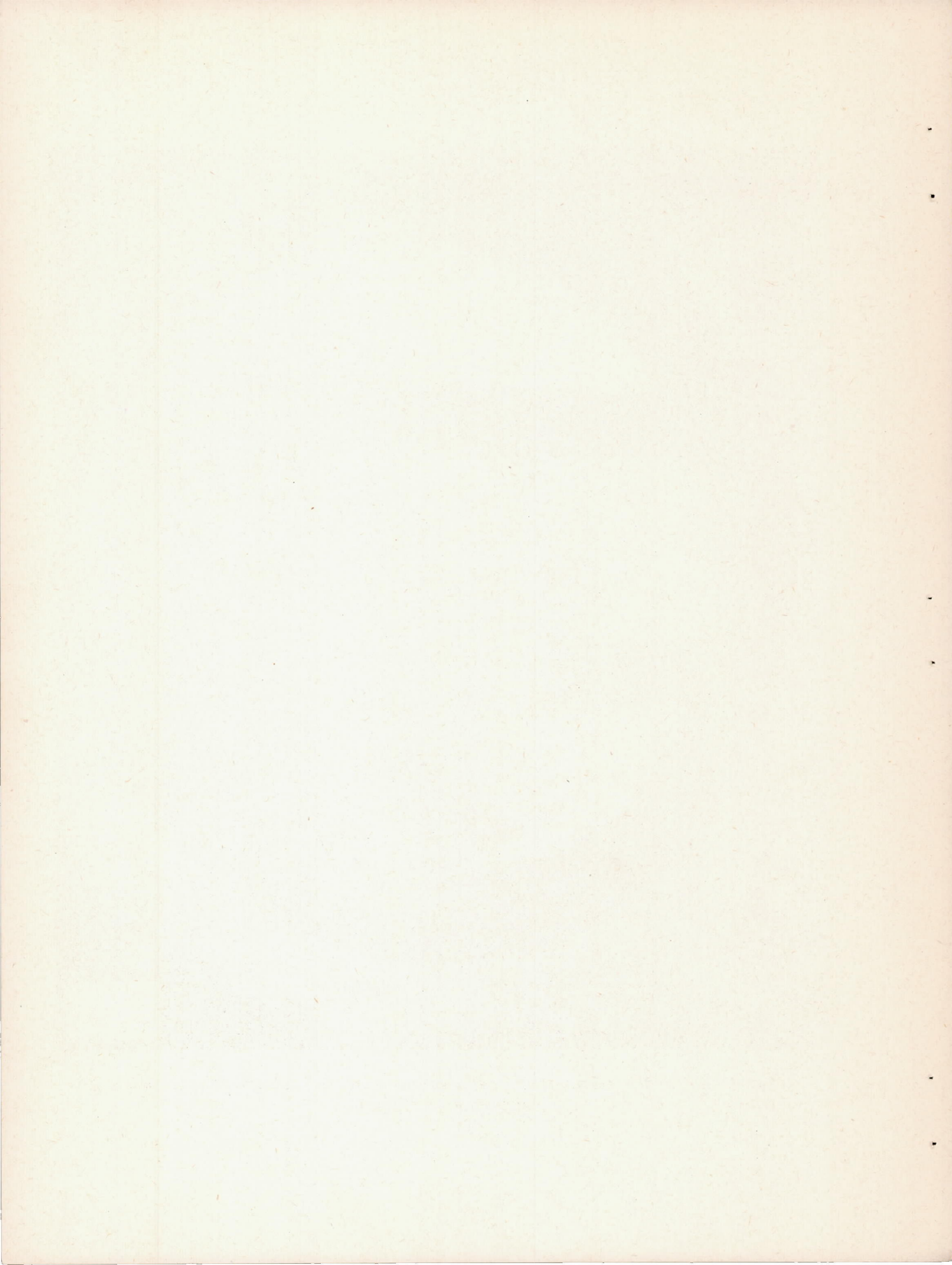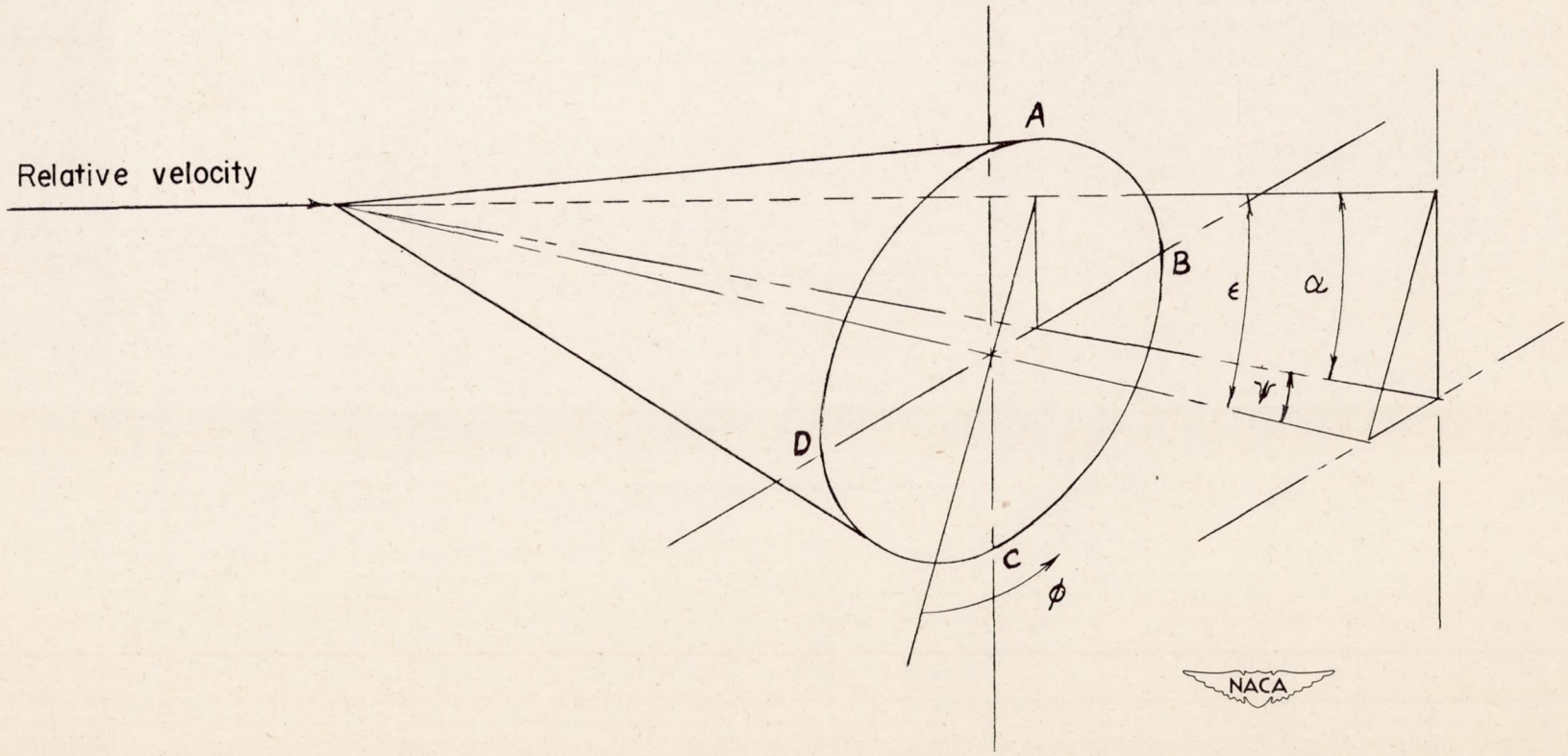
Figure 3.- Orifice installation and angle notation.
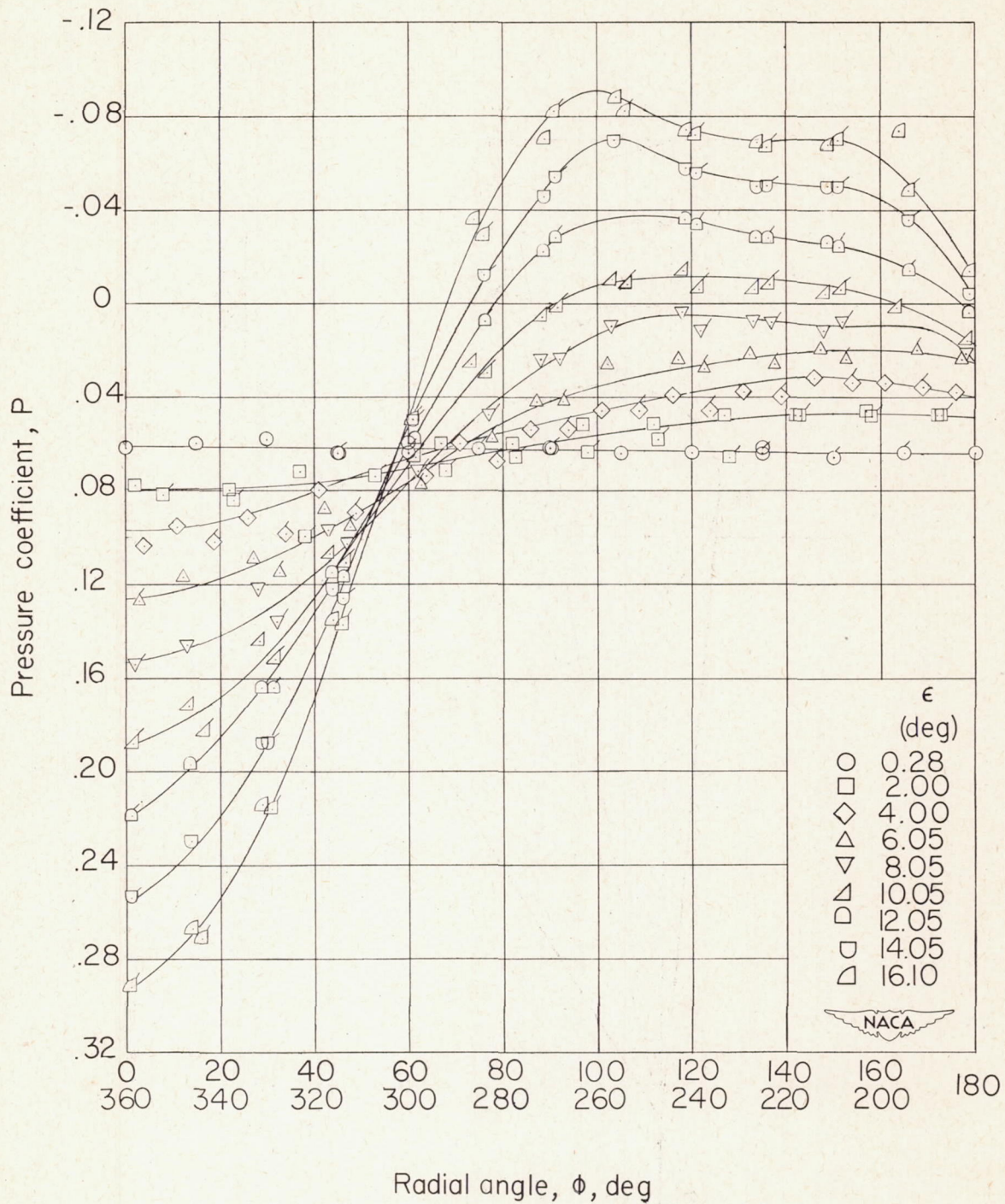
Figure 4.- Radial pressure distributions for representative incidence
angles. Flagged symbols designate values between 180° and 360°.
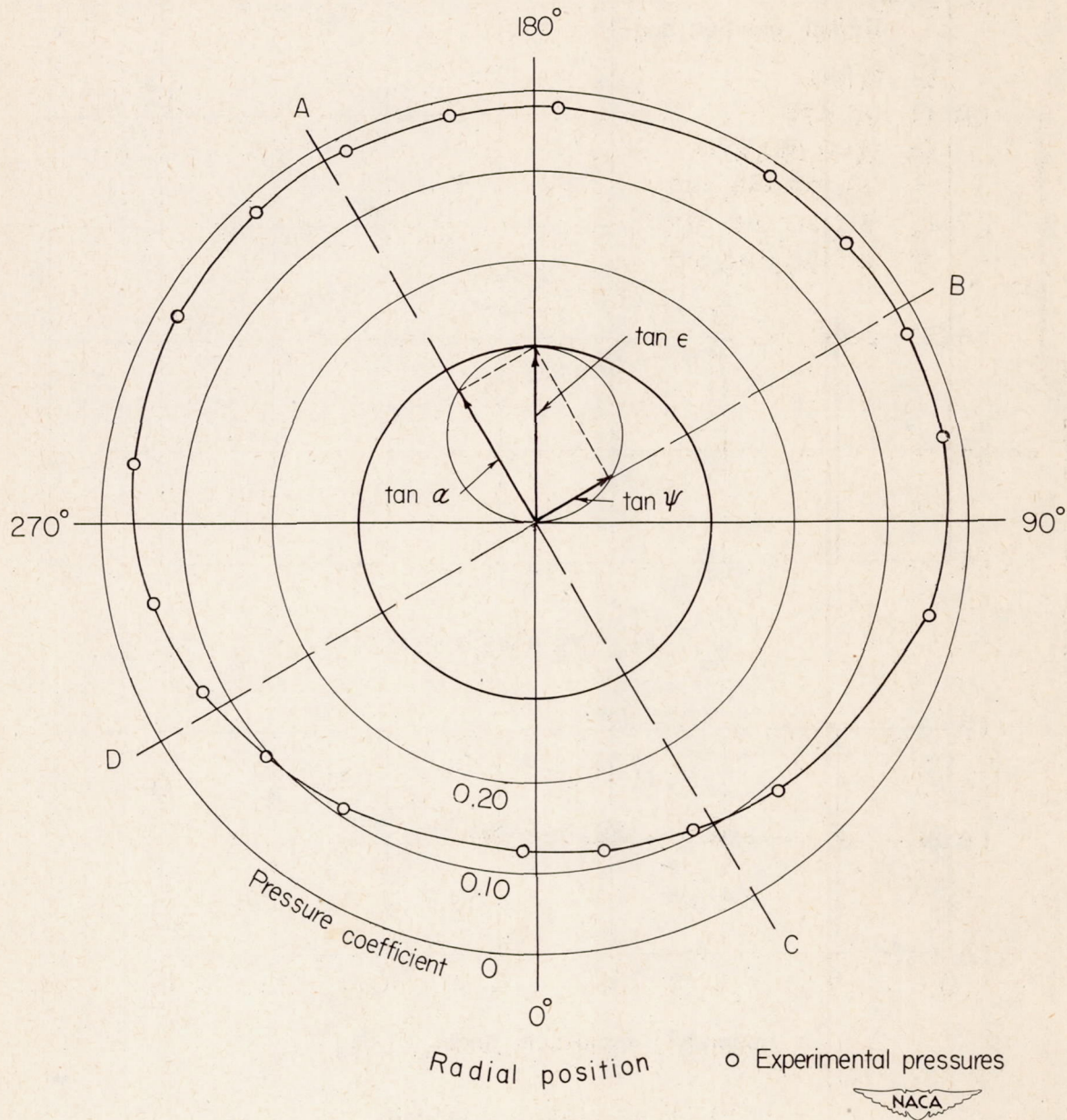
Figure 5.- Resolution of incidence angle to arbitrary combinations
of pitch and yaw for an incidence angle ε of 6°.
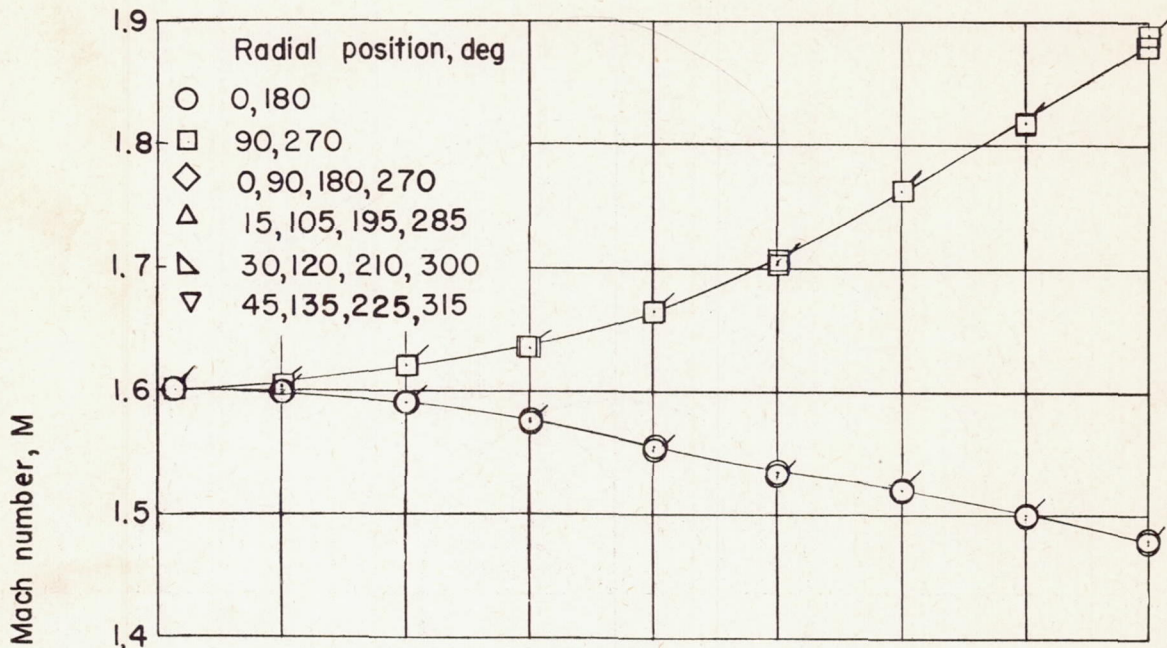
(a) Two static orifices.
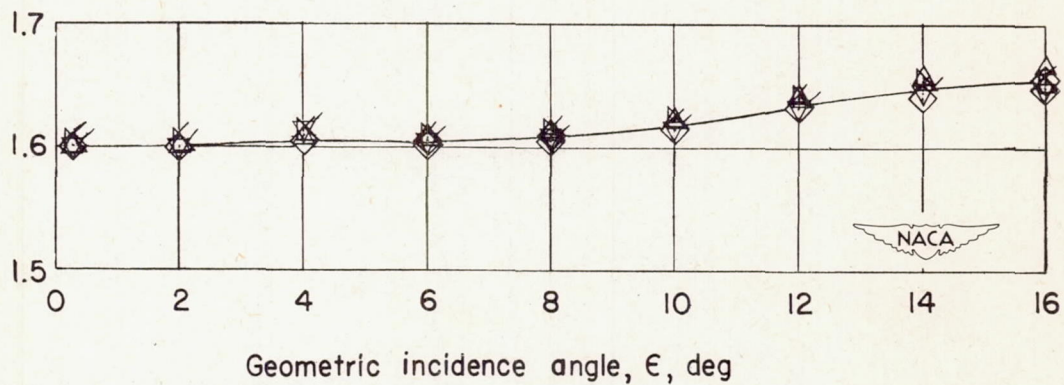
(b) Four static orifices.

Figure 6.- Indicated Mach numbers for two- and four-static-orifice systems
    as a function of geometric incidence angles. Flagged symbols indicate
    Mach numbers based on total pressure for $\epsilon = 0.28^{\circ}$.
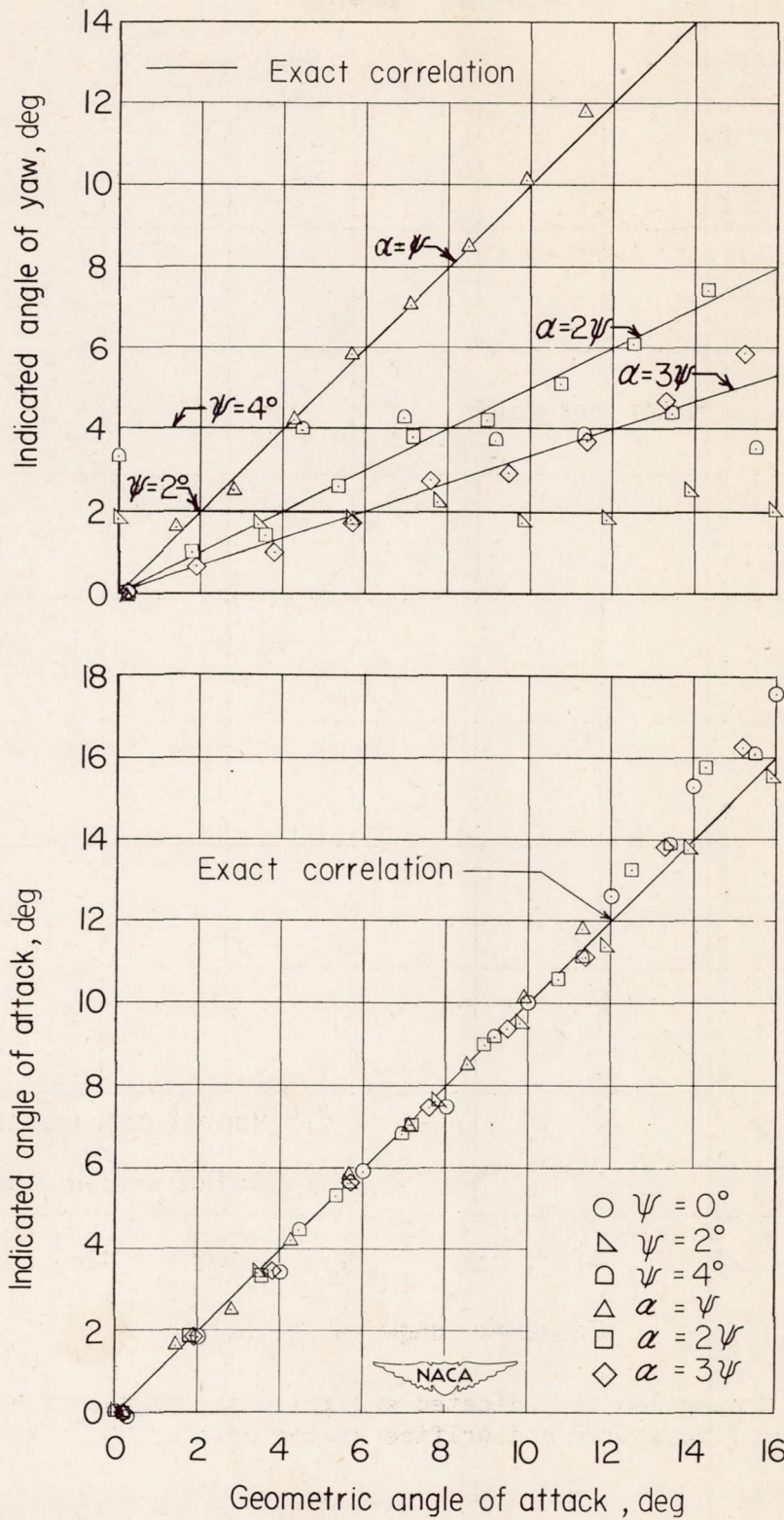
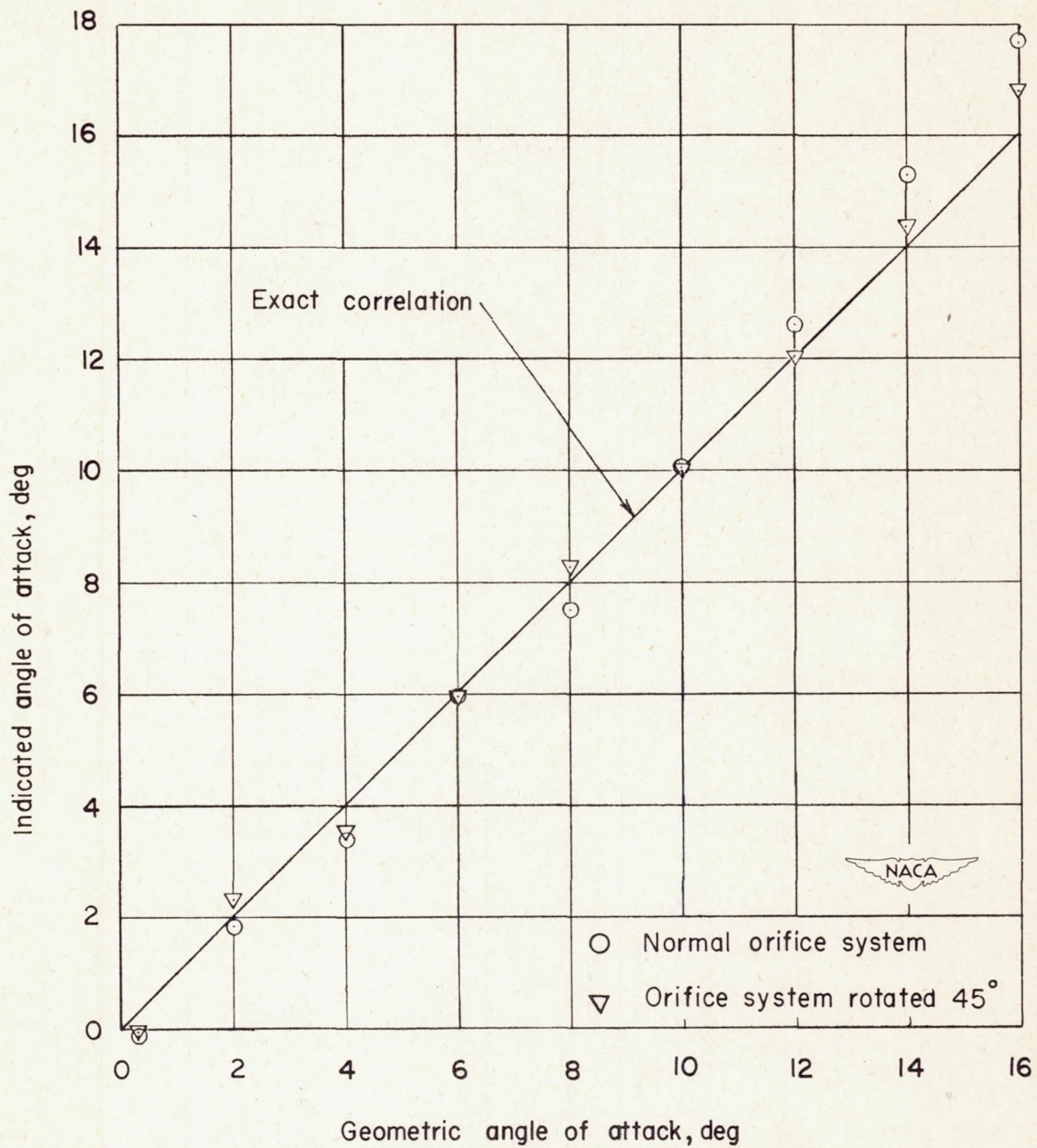Figure 7.- Comparison of indicated and geometric angles of attack and yaw.

Figure 8.- Comparison of indicated and geometric angles of attack for normal orifice system and orifice system rotated 45°. $\psi = 0^\circ$.
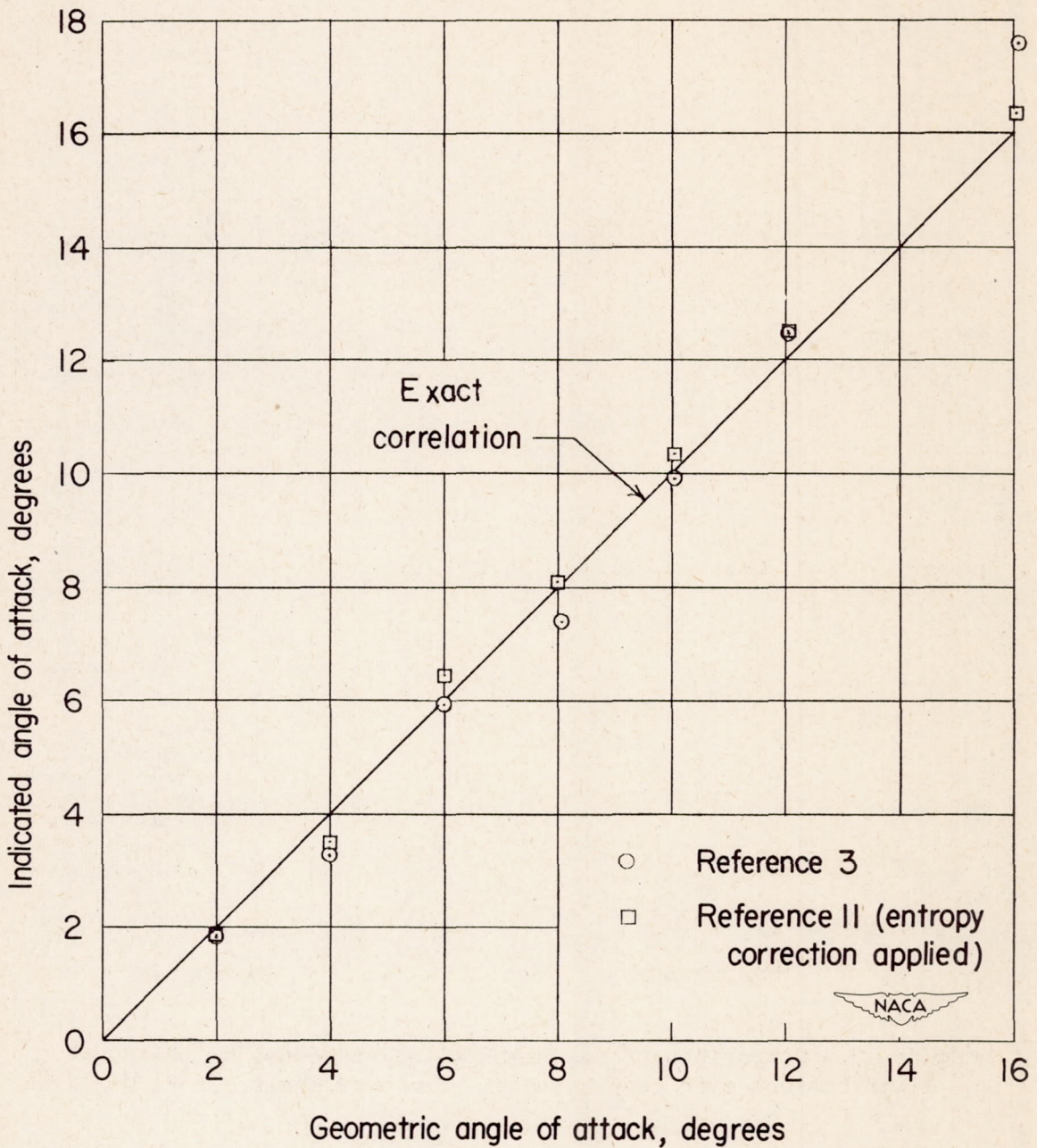
Figure 9.- Comparison of indicated and geometric angles of attack for data reduction based on reference 3 and reference 11 (correction applied). M = 1.60; ψ = 0°.
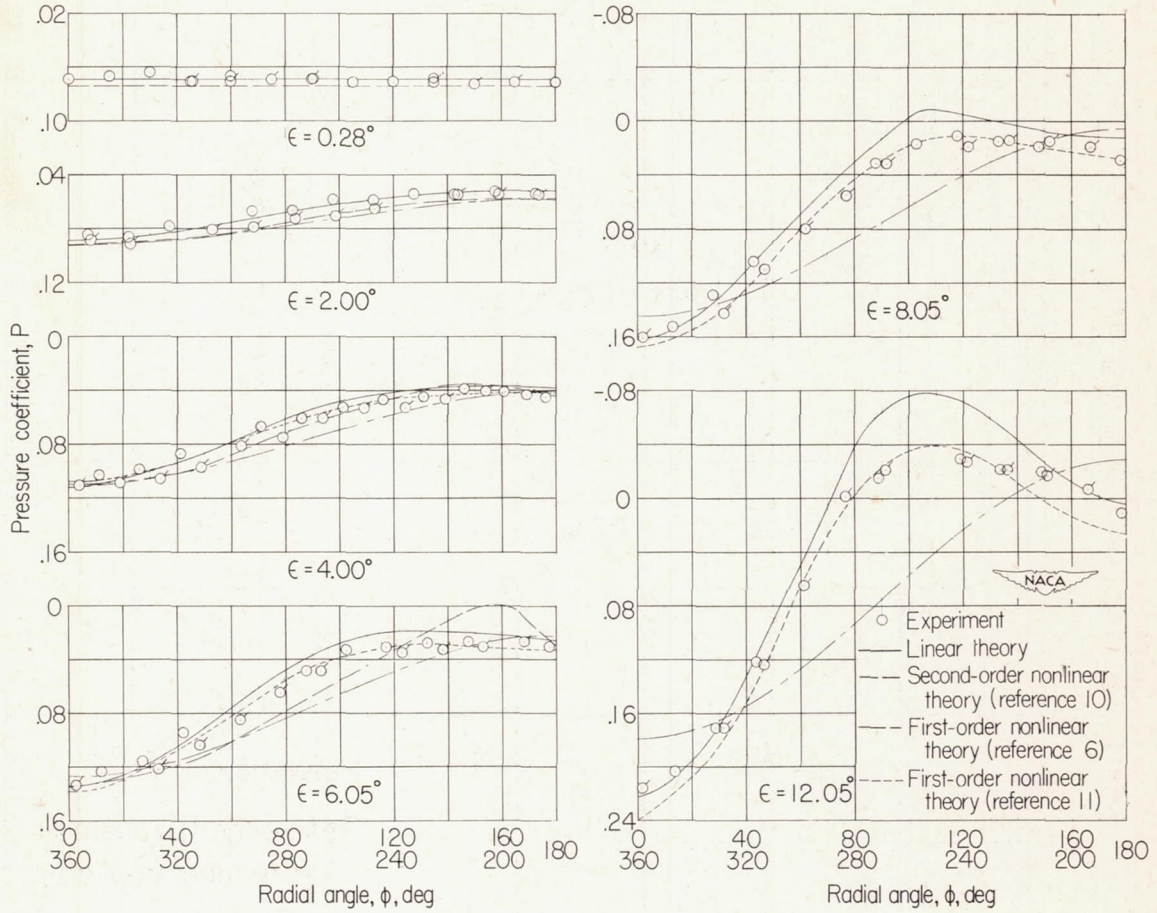
Figure 10.- Comparison of experimental and theoretical pressure
distributions over cone surface. Semiapex angle, 7.5°; M = 1.60.